BABAR-PUB-03/39
SLAC-PUB-10296
hep-ex/0401002

Search for the Rare Leptonic Decay $B^+ \to \mu^+\nu_\mu$

B. Aubert,[1] R. Barate,[1] D. Boutigny,[1] F. Couderc,[1] J.-M. Gaillard,[1] A. Hicheur,[1] Y. Karyotakis,[1] J. P. Lees,[1] V. Tisserand,[1] A. Zghiche,[1] A. Palano,[2] A. Pompili,[2] J. C. Chen,[3] N. D. Qi,[3] G. Rong,[3] P. Wang,[3] Y. S. Zhu,[3] G. Eigen,[4] I. Ofte,[4] B. Stugu,[4] G. S. Abrams,[5] A. W. Borgland,[5] A. B. Breon,[5] D. N. Brown,[5] J. Button-Shafer,[5] R. N. Cahn,[5] E. Charles,[5] C. T. Day,[5] M. S. Gill,[5] A. V. Gritsan,[5] Y. Groysman,[5] R. G. Jacobsen,[5] R. W. Kadel,[5] J. Kadyk,[5] L. T. Kerth,[5] Yu. G. Kolomensky,[5] G. Kukartsev,[5] C. LeClerc,[5] M. E. Levi,[5] G. Lynch,[5] L. M. Mir,[5] P. J. Oddone,[5] T. J. Orimoto,[5] M. Pripstein,[5] N. A. Roe,[5] M. T. Ronan,[5] V. G. Shelkov,[5] A. V. Telnov,[5] W. A. Wenzel,[5] K. Ford,[6] T. J. Harrison,[6] C. M. Hawkes,[6] S. E. Morgan,[6] A. T. Watson,[6] N. K. Watson,[6] M. Fritsch,[7] K. Goetzen,[7] T. Held,[7] H. Koch,[7] B. Lewandowski,[7] M. Pelizaeus,[7] K. Peters,[7] H. Schmuecker,[7] M. Steinke,[7] J. T. Boyd,[8] N. Chevalier,[8] W. N. Cottingham,[8] M. P. Kelly,[8] T. E. Latham,[8] C. Mackay,[8] F. F. Wilson,[8] K. Abe,[9] T. Cuhadar-Donszelmann,[9] C. Hearty,[9] T. S. Mattison,[9] J. A. McKenna,[9] D. Thiessen,[9] P. Kyberd,[10] A. K. McKemey,[10] L. Teodorescu,[10] V. E. Blinov,[11] A. D. Bukin,[11] V. B. Golubev,[11] V. N. Ivanchenko,[11] E. A. Kravchenko,[11] A. P. Onuchin,[11] S. I. Serednyakov,[11] Yu. I. Skovpen,[11] E. P. Solodov,[11] A. N. Yushkov,[11] D. Best,[12] M. Bruinsma,[12] M. Chao,[12] I. Eschrich,[12] D. Kirkby,[12] A. J. Lankford,[12] M. Mandelkern,[12] R. K. Mommsen,[12] W. Roethel,[12] D. P. Stoker,[12] C. Buchanan,[13] B. L. Hartfiel,[13] J. W. Gary,[14] J. Layter,[14] B. C. Shen,[14] K. Wang,[14] D. del Re,[15] H. K. Hadavand,[15] E. J. Hill,[15] D. B. MacFarlane,[15] H. P. Paar,[15] Sh. Rahatlou,[15] V. Sharma,[15] J. W. Berryhill,[16] C. Campagnari,[16] B. Dahmes,[16] S. L. Levy,[16] O. Long,[16] A. Lu,[16] M. A. Mazur,[16] J. D. Richman,[16] W. Verkerke,[16] T. W. Beck,[17] J. Beringer,[17] A. M. Eisner,[17] C. A. Heusch,[17] W. S. Lockman,[17] T. Schalk,[17] R. E. Schmitz,[17] B. A. Schumm,[17] A. Seiden,[17] P. Spradlin,[17] W. Walkowiak,[17] D. C. Williams,[17] M. G. Wilson,[17] J. Albert,[18] E. Chen,[18] G. P. Dubois-Felsmann,[18] A. Dvoretskii,[18] R. J. Erwin,[18] D. G. Hitlin,[18] I. Narsky,[18] T. Piatenko,[18] F. C. Porter,[18] A. Ryd,[18] A. Samuel,[18] S. Yang,[18] S. Jayatilleke,[19] G. Mancinelli,[19] B. T. Meadows,[19] M. D. Sokoloff,[19] T. Abe,[20] F. Blanc,[20] P. Bloom,[20] S. Chen,[20] P. J. Clark,[20] W. T. Ford,[20] U. Nauenberg,[20] A. Olivas,[20] P. Rankin,[20] J. Roy,[20] J. G. Smith,[20] W. C. van Hoek,[20] L. Zhang,[20] J. L. Harton,[21] T. Hu,[21] A. Soffer,[21] W. H. Toki,[21] R. J. Wilson,[21] J. Zhang,[21] D. Altenburg,[22] T. Brandt,[22] J. Brose,[22] T. Colberg,[22] M. Dickopp,[22] E. Feltresi,[22] A. Hauke,[22] H. M. Lacker,[22] E. Maly,[22] R. Müller-Pfefferkorn,[22] R. Nogowski,[22] S. Otto,[22] J. Schubert,[22] K. R. Schubert,[22] R. Schwierz,[22] B. Spaan,[22] D. Bernard,[23] G. R. Bonneaud,[23] F. Brochard,[23] P. Grenier,[23] Ch. Thiebaux,[23] G. Vasileiadis,[23] M. Verderi,[23] D. J. Bard,[24] A. Khan,[24] D. Lavin,[24] F. Muheim,[24] S. Playfer,[24] M. Andreotti,[25] V. Azzolini,[25] D. Bettoni,[25] C. Bozzi,[25] R. Calabrese,[25] G. Cibinetto,[25] E. Luppi,[25] M. Negrini,[25] L. Piemontese,[25] A. Sarti,[25] E. Treadwell,[26] R. Baldini-Ferroli,[27] A. Calcaterra,[27] R. de Sangro,[27] G. Finocchiaro,[27] P. Patteri,[27] M. Piccolo,[27] A. Zallo,[27] A. Buzzo,[28] R. Capra,[28] R. Contri,[28] G. Crosetti,[28] M. Lo Vetere,[28] M. Macri,[28] M. R. Monge,[28] S. Passaggio,[28] C. Patrignani,[28] E. Robutti,[28] A. Santroni,[28] S. Tosi,[28] S. Bailey,[29] M. Morii,[29] E. Won,[29] R. S. Dubitzky,[30] U. Langenegger,[30] W. Bhimji,[31] D. A. Bowerman,[31] P. D. Dauncey,[31] U. Egede,[31] J. R. Gaillard,[31] G. W. Morton,[31] J. A. Nash,[31] G. P. Taylor,[31] G. J. Grenier,[32] S.-J. Lee,[32] U. Mallik,[32] J. Cochran,[33] H. B. Crawley,[33] J. Lamsa,[33] W. T. Meyer,[33] S. Prell,[33] E. I. Rosenberg,[33] J. Yi,[33] M. Davier,[34] G. Grosdidier,[34] A. Höcker,[34] S. Laplace,[34] F. Le Diberder,[34] V. Lepeltier,[34] A. M. Lutz,[34] T. C. Petersen,[34] S. Plaszczynski,[34] M. H. Schune,[34] L. Tantot,[34] G. Wormser,[34] V. Brigljević,[35] C. H. Cheng,[35] D. J. Lange,[35] M. C. Simani,[35] D. M. Wright,[35] A. J. Bevan,[36] J. P. Coleman,[36] J. R. Fry,[36] E. Gabathuler,[36] R. Gamet,[36] M. Kay,[36] R. J. Parry,[36] D. J. Payne,[36] R. J. Sloane,[36] C. Touramanis,[36] J. J. Back,[37] P. F. Harrison,[37] G. B. Mohanty,[37] C. L. Brown,[38] G. Cowan,[38] R. L. Flack,[38] H. U. Flaecher,[38] S. George,[38] M. G. Green,[38] A. Kurup,[38] C. E. Marker,[38] T. R. McMahon,[38] S. Ricciardi,[38] F. Salvatore,[38] G. Vaitsas,[38] M. A. Winter,[38] D. Brown,[39] C. L. Davis,[39] J. Allison,[40] N. R. Barlow,[40] R. J. Barlow,[40] P. A. Hart,[40] M. C. Hodgkinson,[40] G. D. Lafferty,[40] A. J. Lyon,[40] J. C. Williams,[40] A. Farbin,[41] W. D. Hulsbergen,[41] A. Jawahery,[41] D. Kovalskyi,[41] C. K. Lae,[41] V. Lillard,[41] D. A. Roberts,[41] G. Blaylock,[42] C. Dallapiccola,[42] K. T. Flood,[42] S. S. Hertzbach,[42] R. Kofler,[42] V. B. Koptchev,[42] T. B. Moore,[42] S. Saremi,[42] H. Staengle,[42] S. Willocq,[42] R. Cowan,[43] G. Sciolla,[43]

Work supported in part by the Department of Energy contract DE-AC03-76SF00515.

F. Taylor,[43] R. K. Yamamoto,[43] D. J. J. Mangeol,[44] P. M. Patel,[44] S. H. Robertson,[44] A. Lazzaro,[45] F. Palombo,[45] J. M. Bauer,[46] L. Cremaldi,[46] V. Eschenburg,[46] R. Godang,[46] R. Kroeger,[46] J. Reidy,[46] D. A. Sanders,[46] D. J. Summers,[46] H. W. Zhao,[46] S. Brunet,[47] D. Cote-Ahern,[47] P. Taras,[47] H. Nicholson,[48] C. Cartaro,[49] N. Cavallo,[49] G. De Nardo,[49] F. Fabozzi,[49,*] C. Gatto,[49] L. Lista,[49] P. Paolucci,[49] D. Piccolo,[49] C. Sciacca,[49] M. A. Baak,[50] G. Raven,[50] L. Wilden,[50] C. P. Jessop,[51] J. M. LoSecco,[51] T. A. Gabriel,[52] T. Allmendinger,[53] B. Brau,[53] K. K. Gan,[53] K. Honscheid,[53] D. Hufnagel,[53] H. Kagan,[53] R. Kass,[53] T. Pulliam,[53] R. Ter-Antonyan,[53] Q. K. Wong,[53] J. Brau,[54] R. Frey,[54] O. Igonkina,[54] C. T. Potter,[54] N. B. Sinev,[54] D. Strom,[54] E. Torrence,[54] F. Colecchia,[55] A. Dorigo,[55] F. Galeazzi,[55] M. Margoni,[55] M. Morandin,[55] M. Posocco,[55] M. Rotondo,[55] F. Simonetto,[55] R. Stroili,[55] G. Tiozzo,[55] C. Voci,[55] M. Benayoun,[56] H. Briand,[56] J. Chauveau,[56] P. David,[56] Ch. de la Vaissière,[56] L. Del Buono,[56] O. Hamon,[56] M. J. J. John,[56] Ph. Leruste,[56] J. Ocariz,[56] M. Pivk,[56] L. Roos,[56] S. T'Jampens,[56] G. Therin,[56] P. F. Manfredi,[57] V. Re,[57] P. K. Behera,[58] L. Gladney,[58] Q. H. Guo,[58] J. Panetta,[58] F. Anulli,[27,59] M. Biasini,[59] I. M. Peruzzi,[27,59] M. Pioppi,[59] C. Angelini,[60] G. Batignani,[60] S. Bettarini,[60] M. Bondioli,[60] F. Bucci,[60] G. Calderini,[60] M. Carpinelli,[60] V. Del Gamba,[60] F. Forti,[60] M. A. Giorgi,[60] A. Lusiani,[60] G. Marchiori,[60] F. Martinez-Vidal,[60,†] M. Morganti,[60] N. Neri,[60] E. Paoloni,[60] M. Rama,[60] G. Rizzo,[60] F. Sandrelli,[60] J. Walsh,[60] M. Haire,[61] D. Judd,[61] K. Paick,[61] D. E. Wagoner,[61] N. Danielson,[62] P. Elmer,[62] C. Lu,[62] V. Miftakov,[62] J. Olsen,[62] A. J. S. Smith,[62] E. W. Varnes,[62] F. Bellini,[63] G. Cavoto,[62,63] R. Faccini,[63] F. Ferrarotto,[63] F. Ferroni,[63] M. Gaspero,[63] M. A. Mazzoni,[63] S. Morganti,[63] M. Pierini,[63] G. Piredda,[63] F. Safai Tehrani,[63] C. Voena,[63] S. Christ,[64] G. Wagner,[64] R. Waldi,[64] T. Adye,[65] N. De Groot,[65] B. Franek,[65] N. I. Geddes,[65] G. P. Gopal,[65] E. O. Olaiya,[65] S. M. Xella,[65] R. Aleksan,[66] S. Emery,[66] A. Gaidot,[66] S. F. Ganzhur,[66] P.-F. Giraud,[66] G. Hamel de Monchenault,[66] W. Kozanecki,[66] M. Langer,[66] M. Legendre,[66] G. W. London,[66] B. Mayer,[66] G. Schott,[66] G. Vasseur,[66] Ch. Yeche,[66] M. Zito,[66] M. V. Purohit,[67] A. W. Weidemann,[67] F. X. Yumiceva,[67] D. Aston,[68] R. Bartoldus,[68] N. Berger,[68] A. M. Boyarski,[68] O. L. Buchmueller,[68] M. R. Convery,[68] M. Cristinziani,[68] D. Dong,[68] J. Dorfan,[68] D. Dujmic,[68] W. Dunwoodie,[68] E. E. Elsen,[68] R. C. Field,[68] T. Glanzman,[68] S. J. Gowdy,[68] T. Hadig,[68] V. Halyo,[68] T. Hryn'ova,[68] W. R. Innes,[68] M. H. Kelsey,[68] P. Kim,[68] M. L. Kocian,[68] D. W. G. S. Leith,[68] J. Libby,[68] S. Luitz,[68] V. Luth,[68] H. L. Lynch,[68] H. Marsiske,[68] R. Messner,[68] D. R. Muller,[68] C. P. O'Grady,[68] V. E. Ozcan,[68] A. Perazzo,[68] M. Perl,[68] S. Petrak,[68] B. N. Ratcliff,[68] A. Roodman,[68] A. A. Salnikov,[68] R. H. Schindler,[68] J. Schwiening,[68] G. Simi,[68] A. Snyder,[68] A. Soha,[68] J. Stelzer,[68] D. Su,[68] M. K. Sullivan,[68] J. Va'vra,[68] S. R. Wagner,[68] M. Weaver,[68] A. J. R. Weinstein,[68] W. J. Wisniewski,[68] D. H. Wright,[68] C. C. Young,[68] P. R. Burchat,[69] A. J. Edwards,[69] T. I. Meyer,[69] B. A. Petersen,[69] C. Roat,[69] M. Ahmed,[70] S. Ahmed,[70] M. S. Alam,[70] J. A. Ernst,[70] M. A. Saeed,[70] M. Saleem,[70] F. R. Wappler,[70] W. Bugg,[71] M. Krishnamurthy,[71] S. M. Spanier,[71] R. Eckmann,[72] H. Kim,[72] J. L. Ritchie,[72] A. Satpathy,[72] R. F. Schwitters,[72] J. M. Izen,[73] I. Kitayama,[73] X. C. Lou,[73] S. Ye,[73] F. Bianchi,[74] M. Bona,[74] F. Gallo,[74] D. Gamba,[74] C. Borean,[75] L. Bosisio,[75] F. Cossutti,[75] G. Della Ricca,[75] S. Dittongo,[75] S. Grancagnolo,[75] L. Lanceri,[75] P. Poropat,[75,‡] L. Vitale,[75] G. Vuagnin,[75] R. S. Panvini,[76] Sw. Banerjee,[77] C. M. Brown,[77] D. Fortin,[77] P. D. Jackson,[77] R. Kowalewski,[77] J. M. Roney,[77] H. R. Band,[78] S. Dasu,[78] M. Datta,[78] A. M. Eichenbaum,[78] J. R. Johnson,[78] P. E. Kutter,[78] H. Li,[78] R. Liu,[78] F. Di Lodovico,[78] A. Mihalyi,[78] A. K. Mohapatra,[78] Y. Pan,[78] R. Prepost,[78] S. J. Sekula,[78] J. H. von Wimmersperg-Toeller,[78] J. Wu,[78] S. L. Wu,[78] Z. Yu,[78] and H. Neal[79]

(The *BABAR* Collaboration)

[1]*Laboratoire de Physique des Particules, F-74941 Annecy-le-Vieux, France*
[2]*Università di Bari, Dipartimento di Fisica and INFN, I-70126 Bari, Italy*
[3]*Institute of High Energy Physics, Beijing 100039, China*
[4]*University of Bergen, Inst. of Physics, N-5007 Bergen, Norway*
[5]*Lawrence Berkeley National Laboratory and University of California, Berkeley, CA 94720, USA*
[6]*University of Birmingham, Birmingham, B15 2TT, United Kingdom*
[7]*Ruhr Universität Bochum, Institut für Experimentalphysik 1, D-44780 Bochum, Germany*
[8]*University of Bristol, Bristol BS8 1TL, United Kingdom*
[9]*University of British Columbia, Vancouver, BC, Canada V6T 1Z1*
[10]*Brunel University, Uxbridge, Middlesex UB8 3PH, United Kingdom*
[11]*Budker Institute of Nuclear Physics, Novosibirsk 630090, Russia*
[12]*University of California at Irvine, Irvine, CA 92697, USA*
[13]*University of California at Los Angeles, Los Angeles, CA 90024, USA*
[14]*University of California at Riverside, Riverside, CA 92521, USA*
[15]*University of California at San Diego, La Jolla, CA 92093, USA*
[16]*University of California at Santa Barbara, Santa Barbara, CA 93106, USA*

[17]University of California at Santa Cruz, Institute for Particle Physics, Santa Cruz, CA 95064, USA
[18]California Institute of Technology, Pasadena, CA 91125, USA
[19]University of Cincinnati, Cincinnati, OH 45221, USA
[20]University of Colorado, Boulder, CO 80309, USA
[21]Colorado State University, Fort Collins, CO 80523, USA
[22]Technische Universität Dresden, Institut für Kern- und Teilchenphysik, D-01062 Dresden, Germany
[23]Ecole Polytechnique, LLR, F-91128 Palaiseau, France
[24]University of Edinburgh, Edinburgh EH9 3JZ, United Kingdom
[25]Università di Ferrara, Dipartimento di Fisica and INFN, I-44100 Ferrara, Italy
[26]Florida A&M University, Tallahassee, FL 32307, USA
[27]Laboratori Nazionali di Frascati dell'INFN, I-00044 Frascati, Italy
[28]Università di Genova, Dipartimento di Fisica and INFN, I-16146 Genova, Italy
[29]Harvard University, Cambridge, MA 02138, USA
[30]Universität Heidelberg, Physikalisches Institut, Philosophenweg 12, D-69120 Heidelberg, Germany
[31]Imperial College London, London, SW7 2AZ, United Kingdom
[32]University of Iowa, Iowa City, IA 52242, USA
[33]Iowa State University, Ames, IA 50011-3160, USA
[34]Laboratoire de l'Accélérateur Linéaire, F-91898 Orsay, France
[35]Lawrence Livermore National Laboratory, Livermore, CA 94550, USA
[36]University of Liverpool, Liverpool L69 3BX, United Kingdom
[37]Queen Mary, University of London, E1 4NS, United Kingdom
[38]University of London, Royal Holloway and Bedford New College, Egham, Surrey TW20 0EX, United Kingdom
[39]University of Louisville, Louisville, KY 40292, USA
[40]University of Manchester, Manchester M13 9PL, United Kingdom
[41]University of Maryland, College Park, MD 20742, USA
[42]University of Massachusetts, Amherst, MA 01003, USA
[43]Massachusetts Institute of Technology, Laboratory for Nuclear Science, Cambridge, MA 02139, USA
[44]McGill University, Montréal, QC, Canada H3A 2T8
[45]Università di Milano, Dipartimento di Fisica and INFN, I-20133 Milano, Italy
[46]University of Mississippi, University, MS 38677, USA
[47]Université de Montréal, Laboratoire René J. A. Lévesque, Montréal, QC, Canada H3C 3J7
[48]Mount Holyoke College, South Hadley, MA 01075, USA
[49]Università di Napoli Federico II, Dipartimento di Scienze Fisiche and INFN, I-80126, Napoli, Italy
[50]NIKHEF, National Institute for Nuclear Physics and High Energy Physics, NL-1009 DB Amsterdam, The Netherlands
[51]University of Notre Dame, Notre Dame, IN 46556, USA
[52]Oak Ridge National Laboratory, Oak Ridge, TN 37831, USA
[53]Ohio State University, Columbus, OH 43210, USA
[54]University of Oregon, Eugene, OR 97403, USA
[55]Università di Padova, Dipartimento di Fisica and INFN, I-35131 Padova, Italy
[56]Universités Paris VI et VII, Lab de Physique Nucléaire H. E., F-75252 Paris, France
[57]Università di Pavia, Dipartimento di Elettronica and INFN, I-27100 Pavia, Italy
[58]University of Pennsylvania, Philadelphia, PA 19104, USA
[59]Università di Perugia, Dipartimento di Fisica and INFN, I-06100 Perugia, Italy
[60]Università di Pisa, Dipartimento di Fisica, Scuola Normale Superiore and INFN, I-56127 Pisa, Italy
[61]Prairie View A&M University, Prairie View, TX 77446, USA
[62]Princeton University, Princeton, NJ 08544, USA
[63]Università di Roma La Sapienza, Dipartimento di Fisica and INFN, I-00185 Roma, Italy
[64]Universität Rostock, D-18051 Rostock, Germany
[65]Rutherford Appleton Laboratory, Chilton, Didcot, Oxon, OX11 0QX, United Kingdom
[66]DSM/Dapnia, CEA/Saclay, F-91191 Gif-sur-Yvette, France
[67]University of South Carolina, Columbia, SC 29208, USA
[68]Stanford Linear Accelerator Center, Stanford, CA 94309, USA
[69]Stanford University, Stanford, CA 94305-4060, USA
[70]State Univ. of New York, Albany, NY 12222, USA
[71]University of Tennessee, Knoxville, TN 37996, USA
[72]University of Texas at Austin, Austin, TX 78712, USA
[73]University of Texas at Dallas, Richardson, TX 75083, USA
[74]Università di Torino, Dipartimento di Fisica Sperimentale and INFN, I-10125 Torino, Italy
[75]Università di Trieste, Dipartimento di Fisica and INFN, I-34127 Trieste, Italy
[76]Vanderbilt University, Nashville, TN 37235, USA
[77]University of Victoria, Victoria, BC, Canada V8W 3P6
[78]University of Wisconsin, Madison, WI 53706, USA
[79]Yale University, New Haven, CT 06511, USA

(Dated: January 6, 2004)

We have performed a search for the rare leptonic decay $B^+ \to \mu^+\nu_\mu$ with data collected at the $\Upsilon(4S)$ resonance by the *BABAR* experiment at the PEP-II storage ring. In a sample of 88.4 million $B\overline{B}$ pairs, we find no significant evidence for a signal and set an upper limit on the branching fraction $\mathcal{B}(B^+ \to \mu^+\nu_\mu) < 6.6 \times 10^{-6}$ at the 90% confidence level.

PACS numbers: 13.25.Hw, 12.15.Hh, 11.30.Er

The study of the purely leptonic decays $B^+ \to \ell^+\nu_\ell$ ($\ell = e$, μ, or τ) can provide sensitivity to poorly constrained Standard Model (SM) parameters and also act as a probe of new physics. In the SM, these decays proceed through W-boson annihilation with a branching fraction given by

$$\mathcal{B}(B^+ \to \ell^+\nu_\ell) = \frac{G_F^2 m_B m_\ell^2}{8\pi}\left(1 - \frac{m_\ell^2}{m_B^2}\right)^2 f_B^2 |V_{ub}|^2 \tau_{B^+},$$

where G_F is the Fermi coupling constant, m_ℓ and m_B are the lepton and B meson masses, and τ_{B^+} is the B^+ lifetime. The decay rate is sensitive to the product of the Cabibbo-Kobayashi-Maskawa (CKM) matrix element $|V_{ub}|$ and the B decay constant f_B, which is proportional to the wave function for zero separation between the quarks. Currently, our best understanding of f_B comes from lattice gauge calculations where the theoretical uncertainty is roughly 15% [1]. This uncertainty is a significant limitation on the extraction of $|V_{td}|$ from precision $B^0\overline{B}^0$ mixing measurements [2]. Observation of $B^+ \to \ell^+\nu_\ell$ could provide the first direct measurement of f_B.

In this note, we present a search for the decay $B^+ \to \mu^+\nu_\mu$ (charge conjugation is implied throughout this paper). This decay is highly suppressed due to the dependence on $|V_{ub}|^2$ and m_ℓ^2 (helicity suppression). Assuming $|V_{ub}| = 0.0036$ [3] and $f_B = 198$ MeV [1], the SM prediction for the $B^+ \to \mu^+\nu_\mu$ branching fraction is roughly 4×10^{-7}. The current best published limit, from the CLEO collaboration, is $\mathcal{B}(B^+ \to \mu^+\nu_\mu) < 2.1 \times 10^{-5}$ at the 90% confidence level [4].

The $B^+ \to \ell^+\nu_\ell$ decay modes are also potentially sensitive to physics beyond the SM. For example, in two-Higgs-doublet models such as the Minimal Supersymmetric Standard Model (MSSM), these decays can proceed at tree-level via an intermediate $H^\pm$, providing a possible enhancement up to current experimental limits [5]. Similarly, in R-parity violating extensions of the MSSM, $B^+ \to \ell^+\nu_\ell$ may be mediated by scalar supersymmetric particles [6, 7]. Hence, upper limits on the $B^+ \to \ell^+\nu_\ell$ branching fractions constrain the R-parity violating couplings.

The data used in this analysis were collected with the *BABAR* detector at the PEP-II storage ring. The data sample consists of an integrated luminosity of 81.4 fb^{-1} accumulated at the $\Upsilon(4S)$ resonance ("on-resonance") and 9.6 fb^{-1} accumulated at a center-of-mass (CM) energy about 40 MeV below the $\Upsilon(4S)$ resonance ("off-resonance"). The on-resonance sample corresponds to 88.4 million $B\overline{B}$ pairs.

The *BABAR* detector is optimized for the asymmetric collisions at PEP-II and is described in detail elsewhere [8]. Charged particle trajectories are measured with a 5-layer double-sided silicon vertex tracker (SVT) and a 40-layer drift chamber (DCH), which are contained in the 1.5 T magnetic field of a superconducting solenoid. A detector of internally reflected Cherenkov radiation provides identification of charged kaons and pions. The energies of neutral particles are measured by an electromagnetic calorimeter (EMC) consisting of 6580 CsI(Tl) crystals. The flux return of the solenoid is instrumented with resistive plate chambers to provide muon identification (IFR). A Monte Carlo (MC) simulation of the *BABAR* detector based on `GEANT4` [9] was used to optimize the signal selection criteria and evaluate the signal efficiency.

The $B^+ \to \mu^+\nu_\mu$ decay produces a mono-energetic muon in the B rest frame with $p_\mu \approx m_B/2$. Since the neutrino goes undetected, we assume that all remaining particles are associated with the decay of the other B in the event, which we denote the "companion" B. Signal events are selected using the kinematic variables $\Delta E = E_B^* - E_{\rm b}^*$ and energy-substituted mass, $m_{\rm ES} = \sqrt{E_{\rm b}^{*2} - \mathbf{p}_B^{*2}}$ where $\mathbf{p}_B^*$ (E_B^*) is the momentum (energy) of the reconstructed companion B and $E_{\rm b}^*$ is the beam energy, all in the $\Upsilon(4S)$ rest frame. We require $m_{\rm ES}$ to be consistent with the B meson mass, and the energy of the companion B to be consistent with $E_{\rm b}^*$ resulting in $\Delta E \simeq 0$.

To reduce non-hadronic backgrounds, we select events that contain at least four charged tracks and have a normalized second Fox-Wolfram moment [10] less than 0.98. Muon candidates are required to penetrate at least 2.2 interaction lengths of material in the IFR, have a measured penetration within 0.8 interaction lengths of that expected for a muon, and have an associated energy in the EMC consistent with that of a minimum-ionizing particle. The muon track must have at least 12 DCH hits, momentum transverse to the beam axis $p_\perp > 0.1$ GeV/c, and a point of closest approach to the interaction point that is within 10 cm along the beam axis and less than 1.5 cm in the transverse plane. For each muon candidate with momentum between 2.25 and 2.95 GeV/c in the CM frame, we attempt to reconstruct the companion B.

The companion B is formed from all charged tracks satisfying the above criteria regarding the distance of closest approach to the interaction point. It also includes all neutral calorimeter clusters with energy greater than 30 MeV. Particle identification is applied to the charged tracks to identify electrons, muons, kaons and protons and the resulting mass hypotheses are applied to these tracks to improve the ΔE resolution. Events with additional identified leptons from the companion B are discarded since they typically arise from semi-leptonic B or charm decays and indicate the presence of additional neutrinos.

Once the companion B is reconstructed, we calculate the muon momentum in the rest frame of the signal B. We assume the signal B travels in the direction opposite that of the companion B momentum in the $\Upsilon(4S)$ rest frame with a momentum determined by the two-body decay $\Upsilon(4S) \to B^+B^-$. For signal muons, the p_μ distribution peaks at 2.64 GeV/c with an RMS of about 100 MeV/c.

Backgrounds may arise from any process producing charged tracks in the momentum range of the signal muon. The two most significant backgrounds are B semi-leptonic decays involving $b \to u\mu\bar{\nu}$ transitions where the endpoint of the muon spectrum approaches that of the signal, and non-resonant $q\bar{q}$ ("continuum") events where a charged pion is mistakenly identified as a muon. The pion misidentification rate has been studied using a pion control sample taken from $e^+e^- \to \tau^+\tau^-$ events in the data. In the momentum and polar angle region relevant for $B^+ \to \mu^+\nu_\mu$, the misidentification probability is estimated to be 2%. In order for continuum events to populate the signal region of ΔE and $m_{\rm ES}$, there must be significant missing energy due to particles outside the detector acceptance, unreconstructed neutral hadrons, or additional neutrinos. The muon momentum spectrum of the background decreases with increasing momentum so we apply an asymmetric cut about the signal peak, $2.58 < p_\mu < 2.78$ GeV/c.

The continuum background is further suppressed using event-shape variables. These events tend to produce a jet-like event topology whereas $B\overline{B}$ events tend to be spherical. We define a variable, θ^*_T, which is the angle between the muon candidate momentum and the thrust axis of the companion B in the CM frame. For continuum background, $|\cos\theta^*_T|$ peaks sharply near one while the distribution is nearly flat for signal decays. By requiring $|\cos\theta^*_T| < 0.55$, we remove approximately 98% of the continuum background while retaining 54% of the signal decays. We also use the polar angle of the missing momentum vector in the laboratory frame, θ_ν, to discriminate against continuum backgrounds. In continuum events, the missing momentum is often due to particles that were outside the detector acceptance. Therefore, we require $|\cos\theta_\nu| < 0.88$ so that the missing momentum is directed into the detector's fiducial volume.

We select $B^+ \to \mu^+\nu_\mu$ signal candidates with simultaneous requirements on ΔE and $m_{\rm ES}$, thus forming a "signal box" defined by $-0.75 < \Delta E < 0.5$ GeV and $m_{\rm ES} > 5.27$ GeV/c^2. The dimensions of the signal box, as well as the above requirements on p_μ, $|\cos\theta^*_T|$ and $|\cos\theta_\nu|$, were determined using an optimization procedure that finds the combination of cuts that maximizes the quantity $S/\sqrt{S+B}$ where S and B are the signal and background yields in the MC simulation respectively. The signal branching fraction was set to the SM expectation during the optimization procedure. In the MC simulation, 24.5% of signal decays passing all previous cuts fall within the signal box. After applying all selection criteria, the $B^+ \to \mu^+\nu_\mu$ efficiency is determined from the simulation to be (2.24 ± 0.07)%, where the uncertainty is due to MC statistics.

TABLE I: The boundaries of the signal box and various sidebands defined for this analysis.

region	ΔE (GeV)	$m_{\rm ES}$ (GeV/c^2)
signal box	[-0.75, 0.50]	> 5.27
blinding box	[-1.30, 0.70]	> 5.24
fit sideband	[-0.75, 0.50]	[5.10, 5.24]
ΔE sideband (bottom)	[-3.00, -1.30]	> 5.10
ΔE sideband (top)	[0.70, 1.50]	> 5.10

In addition to the signal box, we have defined a slightly larger blinding box and three sideband regions. The boundaries of these regions in the (ΔE, $m_{\rm ES}$) plane are listed in Table I. The data within the blinding box were kept hidden until the analysis was completed in order to avoid the introduction of bias in the event-selection process.

We estimate the background in the signal box assuming that the $m_{\rm ES}$ distribution is described by the ARGUS function [11]. This assumption is consistent with the observed distributions in the MC simulation as well as the data in the ΔE sidebands. The single parameter of the ARGUS function (ζ) is determined from an unbinned maximum likelihood fit using the data in the fit sideband defined in Table I. The ARGUS shape (A) is extrapolated through the signal box and constrained to be zero at the endpoint, which is fixed at $E^*_{\rm b} = 5.29$ GeV/c^2. Figure 1 shows the results of the fit. The expected background is calculated using

$$N_{\rm bkg} = N_{\rm fit} \times \frac{\int_{5.27}^{5.29} A(m_{\rm ES}) dm_{\rm ES}}{\int_{5.10}^{5.24} A(m_{\rm ES}) dm_{\rm ES}} \equiv N_{\rm fit} \times R_{\rm ARGUS} \quad (1)$$

where $N_{\rm fit}$ is the number of events contributing to the fit. The result is $N_{\rm bkg} = 5.0^{+1.8}_{-1.4}$ events. The uncertainty is determined by varying ζ by the $\pm1\sigma$ uncertainty from the fit. In the MC simulation (scaled to the on-resonance luminosity), we find 5.7 ± 0.5 background events in the signal box, in agreement with the data extrapolation. The simulation indicates that the background is primarily continuum, consisting of 57% light-quark ($u\overline{u}$, $d\overline{d}$, $s\overline{s}$), 23% $c\overline{c}$, and 20% $B\overline{B}$ events.

By using the ARGUS function to describe the background $m_{\rm ES}$ distribution, we expect to underestimate the contribution of backgrounds that peak within the blinded

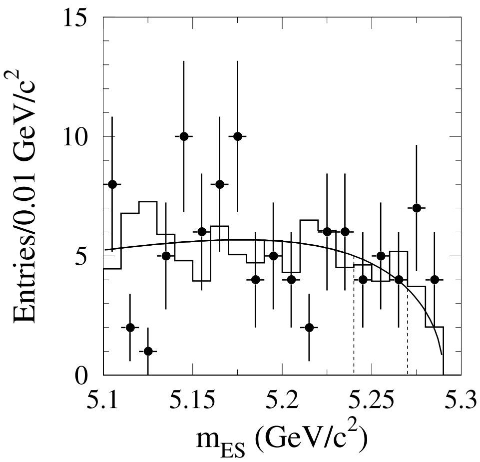

FIG. 1: Results of the ARGUS fit to the on-resonance data satisfying $-0.75 < \Delta E < 0.5$ GeV. The two dashed lines indicate the lower boundaries of the blinded region and signal box at 5.24 GeV/c^2 and 5.27 GeV/c^2, respectively. The fit is performed only on the region $5.10 < m_{\mathrm{ES}} < 5.24$ GeV/c^2 and extrapolated into the signal region to estimate the background. The histogram shows the sum of all simulated background sources normalized to the on-resonance luminosity.

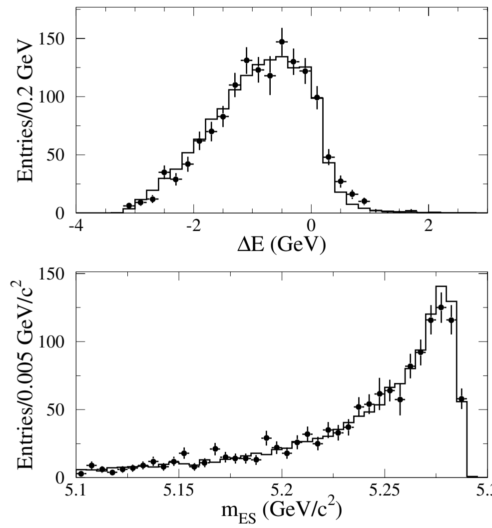

FIG. 2: The distributions of ΔE and m_{ES} of the companion B in the $B^+ \to D^0\pi^+$ control sample after all previous cuts have been applied. The points are the on-resonance data while the histogram is the MC simulation normalized to the number of reconstructed $B^+ \to D^0\pi^+$ decays.

region of m_{ES}. The simulation indicates that only the relatively small component of background due to $B\overline{B}$ events exhibits a mildly peaking m_{ES} distribution. When the background extrapolation is applied to the simulation, the resulting background estimate is 5.2 ± 0.5 events, in agreement with the 5.7 events actually found in the signal box. Although neglecting peaking backgrounds could enhance an apparent signal, here the result would be a more conservative upper limit.

We have evaluated the systematic uncertainty in the signal efficiency which includes the muon candidate selection (particle identification and tracking efficiency) as well as the reconstruction efficiency of the companion B. The muon identification efficiency has been studied using a muon control sample taken from $e^+e^- \to e^+e^-\ \mu^+\mu^-$ events in the data. The identification efficiency is measured in the control sample in bins of momentum, polar angle, and charge, and the results are incorporated into the nominal MC simulation. Due to changing detector conditions, the muon detection efficiency is not stable in time so the simulated events are luminosity-weighted with the correct efficiencies for each run period. Averaged over the momentum and polar angle distributions of muons from $B^+ \to \mu^+\nu_\mu$, we estimate that the muon identification efficiency for this data sample is 61% with a systematic uncertainty of 4.2%. The tracking efficiency of the muon candidate was evaluated from the fraction of tracks reconstructed in the SVT that are also found in the DCH. We find that the tracking efficiency is overestimated in the simulation by 0.8%, which is applied as a correction to the signal efficiency. The associated systematic error is 2%. An additional tracking efficiency systematic error of 1% is included due to the requirement that the event contain at least four charged tracks.

The companion B reconstruction efficiency has been studied using a control sample of fully reconstructed $B^+ \to D^0\pi^+$ and $B^+ \to D^{*0}\pi^+$ events. These are also two-body decays in which the π^+ momentum spectrum is similar to that of the μ^+ in signal events. Once reconstructed, the pion can be treated as if it were the signal muon and the $D^{(*)0}$ decay products can be removed from the event to simulate the unobserved neutrino. Then the companion B is reconstructed in the control sample as it would be for signal. We then compare the efficiencies for each of our companion B selection cuts in the $B^+ \to D^{(*)0}\pi^+$ data and MC simulation. Figure 2 shows a comparison of on-resonance data and simulation for the ΔE and m_{ES} distributions in the $B^+ \to D^0\pi^+$ control sample. We expect the resolution observed in the control sample to represent that of $B^+ \to \mu^+\nu_\mu$ signal events. We find that the efficiency after all selection cuts is lower in the data by a factor of 0.94 ± 0.04 where the uncertainty is due to the statistics of the data and MC control samples. Most of this discrepancy is due to the requirement on m_{ES}. The signal efficiency obtained from the simulation is therefore corrected by this factor and a systematic error of 4.3% is applied. A summary of the systematic uncertainties in the signal efficiency is given in Table II. We estimate the overall signal selection efficiency to be 2.09 ± 0.06 (stat) $\pm$ 0.13 (syst) %.

In the on-resonance data we find 11 events in the signal box where $5.0^{+1.8}_{-1.4}$ background events are expected. The distribution of the data in the (ΔE, m_{ES}) plane is shown in Figure 3. The 90% CL upper limit on the number

TABLE II: Contributions to the systematic uncertainty on the signal efficiency.

source	correction	uncertainty
tracking efficiency		
muon	0.992	2.0%
companion B	-	1.0%
muon identification	-	4.2%
companion B reconstruction	0.94	4.3%
total	0.932	6.4%

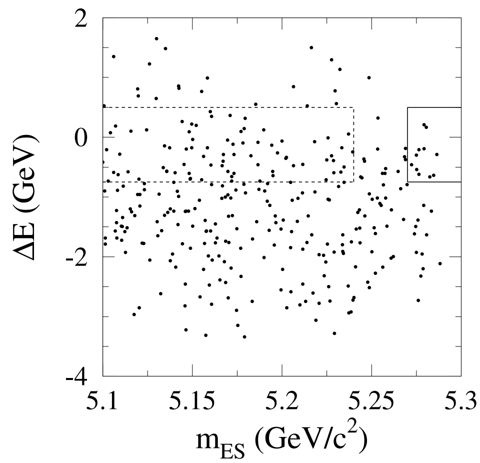

FIG. 3: The distribution of ΔE vs m_{ES} in the on-resonance data after all selection criteria have been applied. The signal box is represented by the solid lines while the dashed lines indicate the region used to estimate the background.

of signal events observed is $n_{UL} = 12.1$ events while the probability of a background fluctuation yielding the observed number of events or more is about 4%. We set an upper limit on the $B^+ \to \mu^+\nu_\mu$ branching fraction using $\mathcal{B}(B^+ \to \mu^+\nu_\mu) < n_{UL}/S$ where S is the sensitivity of the experiment which is the product of the signal efficiency and the number of $B^\pm$ mesons in the sample. Assuming equal production of B^0 and B^+ in $\Upsilon(4S)$ decays, the number of $B^\pm$ mesons in the on-resonance data sample is estimated to be 88.4 million with an uncertainty of 1.1% . Systematic uncertainties are included in the upper limit following the prescription given in reference [12]. We find

$$\mathcal{B}(B^+ \to \mu^+\nu_\mu) < 6.6 \times 10^{-6}$$

at the 90% confidence level.

We are grateful for the excellent luminosity and machine conditions provided by our PEP-II colleagues, and for the substantial dedicated effort from the computing organizations that support *BABAR*. The collaborating institutions wish to thank SLAC for its support and kind hospitality. This work is supported by DOE and NSF (USA), NSERC (Canada), IHEP (China), CEA and CNRS-IN2P3 (France), BMBF and DFG (Germany), INFN (Italy), FOM (The Netherlands), NFR (Norway), MIST (Russia), and PPARC (United Kingdom). Individuals have received support from the A. P. Sloan Foundation, Research Corporation, and Alexander von Humboldt Foundation.

---

* Also with Università della Basilicata, Potenza, Italy
† Also with IFIC, Instituto de Física Corpuscular, CSIC-Universidad de Valencia, Valencia, Spain
‡ Deceased

[1] S. M. Ryan, *Nucl. Phys. Proc. Suppl.* **106**, 86 (2002).
[2] M. Battaglia *et al.*, arXiv:hep-ph/0304132.
[3] Particle Data Group, K. Hagiwara *et al. Phys. Rev.* D **66**, 010001 (2002).
[4] CLEO Collaboration, M. Artuso *et al.*, *Phys. Rev. Lett.* **75**, 785 (1995).
[5] W. S. Hou, *Phys.Rev.* D *Brief Reports* **48**, 2342 (1993).
[6] S. Baek and Y. G. Kim, *Phys. Rev.* D **60**, 077701 (1999).
[7] A. G. Akeroyd and S. Recksiegel, *Phys. Lett.* B **541**, 121 (2002).
[8] *BABAR* Collaboration, A. Palano *et al.*, *Nucl. Instrum. Methods* A **479**, 1 (2002).
[9] S. Agostinelli *et al.* [GEANT4 Collaboration], *Nucl. Instrum. Methods* A **506**, 250 (2003).
[10] G. C. Fox and S. Wolfram, *Phys. Rev. Lett.* **41**, 1581 (1978).
[11] The ARGUS function is defined by

$$\mathcal{A}(m_{\mathrm{ES}}) \propto m_{\mathrm{ES}}\sqrt{1 - {m_{\mathrm{ES}}}^2/E_{\mathrm{b}}^{*2}}\ \exp[-\zeta(1 - {m_{\mathrm{ES}}}^2/E_{\mathrm{b}}^{*2})].$$

ARGUS Collaboration, H. Albrecht *et al.*, *Phys. Lett.* B **241**, 278 (1990).
[12] R. D. Cousins and V. L. Highland, *Nucl. Instrum. Methods* A **320**, 331 (1992).